JOURNAL OF GEOPHYSICAL RESEARCH, VOL. 108, NO. D3, 4128, doi:10.1029/2002JD002717, 2003

Annual cycle of global distributions of aerosol optical depth from integration of MODIS retrievals and GOCART model simulations

Hongbin Yu, R. E. Dickinson, and M. Chin[1]
School of Earth and Atmospheric Sciences, Georgia Institute of Technology, Atlanta, Georgia, USA

Y. J. Kaufman
Laboratory for Atmospheres, NASA Goddard Space Flight Center, Greenbelt, Maryland, USA

B. N. Holben
Biospheric Sciences Branch, NASA Goddard Space Flight Center, Greenbelt, Maryland, USA

I. V. Geogdzhayev and M. I. Mishchenko
NASA Goddard Institute for Space Studies, New York, USA

Received 3 July 2002; revised 17 September 2002; accepted 30 September 2002; published 14 February 2003.

[1] The Moderate-Resolution Imaging Spectroradiometer (MODIS) instrument onboard the Earth Observing System (EOS) satellites provides an unprecedented opportunity to study aerosols from space with high accuracy and on a nearly global scale. However, difficulty with highly reflective arid and snow-covered lands introduces significant gaps in global or regional coverage that must be filled by some other means. This study provides a complete global coverage of an annual cycle of aerosol optical depth by combining the MODIS retrievals and Georgia Tech/Goddard Global Ozone Chemistry Aerosol Radiation and Transport (GOCART) simulations weighted with the uncertainties in each product. The assimilated aerosol optical depths over land are better correlated with the ground-based Aerosol Robotic Network (AERONET) measurements than are either the MODIS retrievals or the GOCART simulations alone. The gaps in the MODIS retrievals are filled with values that are generally consistent with the AERONET aerosol climatology. The assimilated aerosol optical depths are in good agreement with the Advanced Very High Resolution Radiometer (AVHRR) aerosol climatology over the Atlantic and North Indian Oceans. In spring, large discrepancies between the MODIS retrievals in 2001 and the AVHRR climatology over the North Pacific are likely a result of extremely active transcontinental transport of Asian dust/pollutants to North America in the year 2001. Large model–satellite differences in the South Pacific and South Indian Oceans may be attributable to missing or underestimated sources in the model and/or cloud, whitecap, and glint contamination in satellite retrievals. *INDEX TERMS:* 0305 Atmospheric Composition and Structure: Aerosols and particles (0345, 4801); 0345 Atmospheric Composition and Structure: Pollution—urban and regional (0305); 0365 Atmospheric Composition and Structure: Troposphere—composition and chemistry; 1640 Global Change: Remote sensing; 3337 Meteorology and Atmospheric Dynamics: Numerical modeling and data assimilation

Citation: Yu, H., R. E. Dickinson, M. Chin, Y. J. Kaufman, B. N. Holben, I. V. Geogdzhayev, and M. I. Mishchenko, Annual cycle of global distributions of aerosol optical depth from integration of MODIS retrievals and GOCART model simulations, *J. Geophys. Res.*, *108*(D3), 4128, doi:10.1029/2002JD002717, 2003.

1. Introduction

[2] Tropospheric aerosols have a variety of natural and anthropogenic sources. They are relatively short-lived in the atmosphere, with an average residence time of a few days, and are heterogeneous in space and time. They modify radiative fluxes directly by scattering and absorption [*Bohren and Huffman*, 1983; *Coakley et al.*, 1983] and indirectly by acting as cloud condensation nuclei and by changing cloud properties [*Twomey*, 1977; *Albrecht*, 1989; *Rosenfeld*, 1999, 2000]. Their effects on temperature, hence atmospheric stability, further influence clouds and so feedback on the radiation [*Hansen et al.*, 1997; *Ackerman et al.*, 2000]. Consequently, they influence land–air interactions and the

[1]Also at NASA Goddard Space Flight Center, Greenbelt, Maryland, USA.

0148-0227/03/2002JD002717

atmospheric boundary layer [*Yu et al.*, 2002]. They affect global surface air temperatures [*Charlson et al.*, 1992; *Penner et al.*, 1992; *Kiehl and Briegleb*, 1993; *Hansen et al.*, 1997; *Ramanathan et al.*, 2001], photochemistry [*Dickerson et al.*, 1997], and ecosystems [*Chameides et al.*, 1999].

[3] It remains difficult to characterize the large spatial and temporal variations of aerosol properties and hence to estimate their radiative forcing [*Haywood and Boucher*, 2000], and so integrated research is required with multiple platforms and techniques (e.g., ground-based networks, aircraft, ship, satellite remote sensing, and computer modeling) [*Penner et al.*, 1994; *Heintzenberg et al.*, 1996; *Kaufman et al.*, 2002]. Past aerosol retrievals have used the satellite data from operational sensors, e.g., Advanced Very High Resolution Radiometer (AVHRR) and Total Ozone Mapping Spectrometer (TOMS), among others, that were not originally designed for aerosol research. However, they have provided multidecadal climatology that significantly advanced the understanding of aerosol distributions. The newly launched NASA Earth Observing System (EOS) satellite Terra and its successor Aqua carry a sensor designed specifically for aerosol remote sensing, namely the Moderate-Resolution Imaging Spectroradiometer (MODIS), a 36-band well-calibrated spectroradiometer with moderate spatial resolution (250–1000 m) [*King et al.*, 1999]. It provides separate aerosol optical depths for the fine mode and the coarse mode, and applies a new "dark-target" method to obtain aerosol properties with unprecedented accuracy, even over vegetated lands [*Kaufman et al.*, 1997]. However, difficulty with highly reflective arid and snow-covered land introduces large uncertainties and gaps in global or regional coverage that must be filled by some other means.

[4] This study aims to develop an annual cycle of aerosol optical depth with complete global coverage and reasonable accuracy for studies of aerosol induced environmental changes on global or regional scale. For this, aerosol simulations from the Georgia Tech/Goddard Global Ozone Chemistry Aerosol Radiation and Transport (GOCART) model [*Chin et al.*, 2002] are combined with the MODIS retrievals [*Kaufman et al.*, 1997; *Tanre et al.*, 1997]. Both the retrievals and simulations have significant uncertainties, so they are combined by optimum interpolation using an approach similar to that developed for the Indian Ocean Experiment (INDOEX) study [*Collins et al.*, 2001].

[5] Section 2 gives an overview of aerosol data and modeling and a description of the assimilation approach. The geographical patterns and annual variations of assimilated aerosol optical depth are described in section 3, and in section 4, evaluated against Sun photometer measurements from ground-based Aerosol Robotic Network (AERONET) [*Holben et al.*, 2001] and compared with the two-channel AVHRR aerosol climatology [*Mishchenko et al.*, 1999; *Geogdzhayev et al.*, 2002] (M. I. Mishchenko et al., Aerosol retrievals from AVHRR radiances: Effects of particle nonsphericity and absorption and an updated long-term global climatology of aerosol properties, submitted to *Journal of Quantitative Spectroscopy and Radiative Transfer*, 2002, hereinafter referred to as Mishchenko et al., submitted manuscript, 2002). Uncertainties of the aerosol assimilation resulting from assumptions are addressed in section 5 and major conclusions are summarized in section 6.

2. Description of Aerosol Data, Model, and Assimilation Approach

2.1. Aerosol Data and Simulations

2.1.1. MODIS Retrievals

[6] The MODIS instrument onboard the EOS Terra satellite, has been acquiring modest resolution, spectral measurements of aerosol properties over both land and ocean with near daily global coverage since late February 2000 [*King et al.*, 1999]. Terra passes over at 1000–1130 local time. The data have been extensively validated. Prelaunched and postlaunched MODIS aerosol validations show an unprecedentedly high accuracy with uncertainty of $\pm 0.05 \pm 0.20\tau$ for optical depth over land and $\pm 0.03 \pm 0.05\tau$ over ocean [*Kaufman et al.*, 1997; *Tanre et al.*, 1997; *Chu et al.*, 2002; *Remer et al.*, 2002]. This study uses monthly aerosol optical depths at 550 nm for the period from November 2000 to October 2001. The aerosol retrievals are gridded onto a $1^\circ \times 1^\circ$ mesh and mapped into the GOCART $2.5^\circ \times 2.0^\circ$ grid.

2.1.2. GOCART Simulations

[7] The GOCART is a global three-dimensional chemistry-transport model, integrated on a mesh of 2.5° in longitude by 2° in latitude and with 30 layers in the vertical. It is driven by the assimilated meteorological fields from the Goddard Earth Observing System Data Assimilation System (GEOS DAS) [*Chin et al.*, 2000a]. Emissions include sulfate precursors (SO_2 and dimethylsulfide), organic carbon, black carbon, size-resolvable mineral dusts and sea-salt particles. Within the GOCART, aerosol particles and their precursors undergo advection, turbulent mixing, moist convection, dry deposition, wet removal, and chemical transformation [*Chin et al.*, 2000a, 2000b, 2002; *Ginoux et al.*, 2001]. Concentrations of aerosol components are calculated and the aerosol optical depth at 550 nm is derived for an external mixture of the individual components [*Chin et al.*, 2002]. A comparative study [*Chin et al.*, 2002] has shown that the GOCART model captures most of the prominent features of geographical and temporal variations of aerosol optical depths as observed by the TOMS and AVHRR, with no known overall biases compared to the satellite retrievals and AERONET Sun photometer measurements [*Chin et al.*, 2002]. In this study, the monthly averaged GOCART model results from November 2000 to October 2001 are used, the same time period as the MODIS data used here.

2.1.3. AERONET Measurements

[8] The AERONET program is an inclusive federation of ground-based aerosol network equipped well-calibrated Sun photometers, established and maintained by international agencies, institutes, and universities, and composed of more than 100 field sites around the world [*Holben et al.*, 1998]. It provides relatively long-term spectral properties of aerosols for both process studies and aerosol validations [e.g., *Holben et al.*, 2001; *Chin et al.*, 2002; *Chu et al.*, 2002; *Dubovik et al.*, 2002]. Its archived quality-assured monthly aerosol optical depths and Angstrom exponents are used in this study to examine the aerosol assimilation over land.

2.1.4. AVHRR Two-Channel Retrievals

[9] The AVHRR flown on a series of NOAA polar orbiting satellites since 1978 provides an aerosol climatology over the global oceans [*Husar et al.*, 1997]. Its early one-channel aerosol retrievals had significant uncertainties and/or biases because of the inadequacy of simplified aerosol models for characterizing strong temporal and spatial variability of tropospheric aerosols [*Ignatov et al.*, 1995]. Recently several two-channel retrieval algorithms have been developed to improve the accuracy and reduce the bias of AVHRR aerosol retrievals [*Higurashi and Nakajima*, 1999; *Mishchenko et al.*, 1999; *Geogdzhayev et al.*, 2002]. The 1985–1999 AVHRR climatology (Mishchenko et al., submitted manuscript, 2002) is used here. Subsequent years have not yet been retrieved. Although not obtained for the same time period as the MODIS and GOCART aerosols, thus not ideal for a quantitative evaluation, these aerosols are helpful for interpreting the MODIS–GOCART discrepancies. Large effects of the Pinatubo eruptions are removed here by subtracting stratospheric aerosol optical depths [*Sato et al.*, 1993] from the 1991–1993 AVHRR retrievals.

2.1.5. Intercomparisons and Discussion

[10] Figure 1 shows correlations of MODIS retrievals and GOCART simulations with about 400 concurrent monthly observations at about 70 AERONET sites from November 2000 to October 2001. The MODIS retrievals and GOCART simulations have the same resolution of 2.5° × 2°. The dotted line represents a 1:1 relationship. The AERONET measurements were chosen only when the MODIS retrievals are available. The correlation coefficient with respect to AERONET measurements is 0.54 and 0.61 for MODIS and GOCART, respectively. At low optical depths, those from GOCART have no systematic bias compared to AERONET data, but the MODIS values have a high bias. This bias was found in previous MODIS validations and possibly explained by large residuals from surface contributions or instrument signal-to-noise issues [*Chu et al.*, 2002; *Remer et al.*, 2002]. At large optical depths (e.g., $\tau > 0.4$), however, AERONET has a high bias, at least partially associated with the regional siting of AERONET measurements. We find that the AERONET sites with a τ greater than 0.4 are usually close to source regions. Some such sites are situated in cities (e.g., Beijing, Xianghe, Mexico City, Philadelphia, and GSFC) or on islands (e.g., NCU-Taiwan, Shirahama, Okinawa, and Noto). When the 10 × 10 km MODIS data for April 2001 is averaged over different sized boxes centered at the AERONET sites (e.g., Beijing, Xianghe, NCU-Taiwan, and Okinawa), these spatially averaged aerosol optical depths decrease consistently with an increasing averaging area (from 0.4° × 0.4° to 2.4° × 2.4°). In particular, the aerosol optical depth averaged over a 0.4° × 0.4° box is 28–54% higher than that averaged over a 2.4° × 2.4° box. Evidently, the AERONET measurements in these locations should show larger values of aerosol optical depth than those of the surrounding regions.

[11] The different data sets are inconsistent in other ways. The monthly GOCART aerosol is an ensemble of all conditions, covering daytime and nighttime, clear-sky and cloudy-sky, but the composite optical depths from MODIS and AERONET are for clear-sky only, either around noon-time (MODIS) or for a spectrum of daylight hours (AERONET). Diurnal variations of aerosols may be significant in some places, due to a combination of variations of emissions, meteorological processes (especially wind and moisture), and photochemical reactions. Nevertheless, the MODIS measurements on Terra on average well represent the daily aerosols [*Kaufman et al.*, 2000]. Clouds can act as either a source of aerosols through in-cloud aqueous production and near-cloud particle nucleation, or as a sink of aerosols through scavenging and rainout. Through water uptake, particles and hence their extinction can be larger under cloudy than clear sky. The net effect of clouds would be either positive or negative and is scenario dependent [*Hegg*, 2001]. Therefore, this study neglects potential biases resulted from aerosol diurnal variations and cloud processes. Finally, both satellite and surface networks measure the composite of tropospheric and stratospheric aerosols. Although not calculated by GOCART, the optical depth of stratospheric background aerosols is much smaller than that of tropospheric aerosols [*Sato et al.*, 1993] and will not contribute significantly to major differences between observation and simulation.

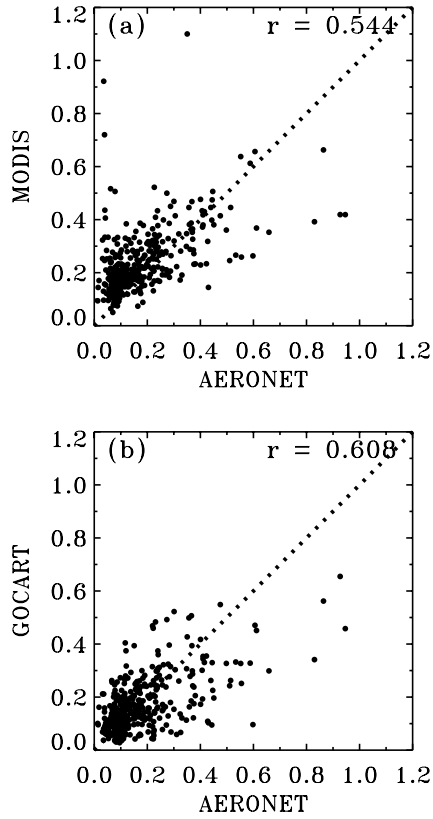

Figure 1. Correlation of (a) MODIS and (b) GOCART monthly aerosol optical depths with the AERONET measurements from November 2000 to October 2001. The dotted line represents a 1:1 relationship.

2.2. Approach of Aerosol Assimilation

[12] The goal of data assimilation or objective analysis is to minimize the misfit between individual descriptions (e.g., modeling and satellite remote sensing) and to form an

optimal estimate of states of the system (e.g., aerosol optical depth), by combining them with weights inversely proportional to the square of errors for individual descriptions [e.g., *Lorenc*, 1986]. This study uses such an optimum interpolation approach with the Kalman–Bucy filter that has been previously applied to assimilations of trace gases [*Levelt et al.*, 1998; *Khattatov et al.*, 1999, 2000; *Lamarque et al.*, 1999] and aerosols [*Collins et al.*, 2001; *Rasch et al.*, 2001]. The assimilation package obtained from http://www.acd.ucar.edu/boris/ (courtesy Dr. Boris Khattatov of NCAR) is adapted to diagnostically derive global distributions of monthly aerosol optical depth from archived MODIS retrievals and GOCART simulations.

[13] Ideally, the assimilation approach requires unbiased observations and simulations. The MODIS retrievals may have been biased in specific regions or everywhere from cloud contamination and/or unrealistic aerosol models, and over oceans from glint and whitecap effects. Modeling biases may result from uncertainties in estimated emissions and aerosol processes and their simplified parameterizations. However, such biases can not currently be quantified or removed. Statistical parameters characterizing the magnitude and propagation of uncertainties are needed for the aerosol assimilation, including fractional error coefficients (f), minimum root-mean-square (RMS) errors (ϵ), and correlation lengths (L). At a single point, the parameter used to weight the relative contributions of the MODIS and GOCART products is their error variances, i.e., $\epsilon^2 + (f\tau)^2$. The correlation of errors between two points is assumed to be a Gaussian function with a characteristic scale of L.

[14] Table 1 specifies values of these parameters for the standard assimilation. For MODIS optical depth, f and ϵ, depending on land and ocean, are determined on the basis of MODIS validations (see section 2.1.1) [*Kaufman et al.*, 1997; *Tanre et al.*, 1997; *Chu et al.*, 2002; *Remer et al.*, 2002]. MODIS is a nadir-pointing satellite instrument with an instantaneous field-of-view of 250–500 m. To first approximation, we assume that errors in the retrieval for adjacent pixels are not correlated, i.e., $L_{obs} = 0$ km. We set $L_{mod} = 200$ km, based on the data analysis of the Lidar In-Space Technology Experiment (LITE) [*Charlson*, 2000]. As such, for a separation of about $3L_{mod}$ between two grids, the model errors are correlated by only 0.1. The agreement between GOCART and AERONET products is generally within a factor of 2, as shown in Figure 1 [*Chin et al.*, 2002]. However, a stringent derivation of GOCART error parameters remains a complicated issue. In this study we assume zero RMS error and the fractional error coefficient of 0.5 for GOCART optical depth on the global basis. The somewhat arbitrary assumption that the minimum RMS errors of modeling are negligible (e.g., $\epsilon_{mod} = 0$) will generally result in a smaller variance and hence a larger weight given to model simulations in remote pristine areas, compared to the MODIS aerosol measurements, though f_{mod} is much larger than f_{obs}. In regions without MODIS retrievals, the assimilation is determined entirely by the GOCART simulations. Elsewhere, the MODIS retrievals usually take a larger weight than the GOCART simulations. These parameters may vary geographically. Sensitivity tests are performed in section 5 to examine potential impacts of such uncertainties on the aerosol assimilation. In all these sensitivity tests, the uncertainty for aerosol optical depth is measured as a relative difference, which is defined as

Table 1. Free Parameters Assigned in the Standard Aerosol Assimilation

Variable	Symbol	Value
Fractional error coefficient in model τ	f_{mod}	0.5
Fractional error coefficient in observational τ	f_{obs}	0.20 (land) 0.05 (ocean)
Minimum RMS error in model τ	ε_{mod}	0.0
Minimum RMS error in observational τ	ε_{obs}	0.05 (land) 0.03 (ocean)
Horizontal correlation length for errors in model τ	L_{mod}	200 km
Horizontal correlation length for errors in observation τ	L_{obs}	0 km

$$\textit{Relative difference}(\%) = \left[\frac{\tau_{sensitivity}}{\tau_{standard}} - 1\right] 100\% \qquad (1)$$

where $\tau_{standard}$ and $\tau_{sensitivity}$ denotes the assimilated aerosol optical depth for standard assimilation and sensitivity test, respectively.

[15] Clearly use of all the 10 km MODIS aerosol retrievals over the globe would require a large amount of CPU time and memory and is currently impractical. As a compromise between reasonable computational efficiency and adequate spatial resolution, the $2.5^\circ \times 2^\circ$ MODIS data are used for the Northern Hemisphere and source/outflow regions in the Southern Hemisphere where the gradient of τ is usually large. For other regions with a relatively small gradient of τ, only every other data point is used. This assumption introduces an uncertainty of at most 15% in the aerosol optical depth in limited areas but reduces the CPU time by about a factor of 3, compared to that of using full $2.5^\circ \times 2^\circ$ MODIS data globally.

3. The Annual Cycle of Global Aerosol Optical Depth

[16] The monthly averages of GOCART simulations are combined with the MODIS monthly aerosol optical depth from November 2000 to October 2001. The assimilated annual cycle of global aerosol optical depth is shown in Figure 2. The geographical patterns and seasonal variations of aerosol optical depth are as follows:

1. North Africa. The aerosol optical depth in North Africa is among the highest in the world throughout the year, a combined effect of biomass burning near the equator and dust outbreaks in the Saharan deserts. The burning of tropical savannas emits a large amount of carbonaceous aerosols during winter and spring, elevating the aerosol optical depth to more than 0.4 over tropical Africa near the west coast, and to more than 0.2 over the whole tropical Atlantic. The relatively high values up to 1 and large extent extending southward in January and February, are consistent with the seasonality of biomass burning in the region [*Delmas et al.*, 1991]. When dust outbreaks occur from the Saharan deserts starting in the spring [*Torres et al.*, 2002], the aerosol optical depth in northern Africa is elevated substantially. These large

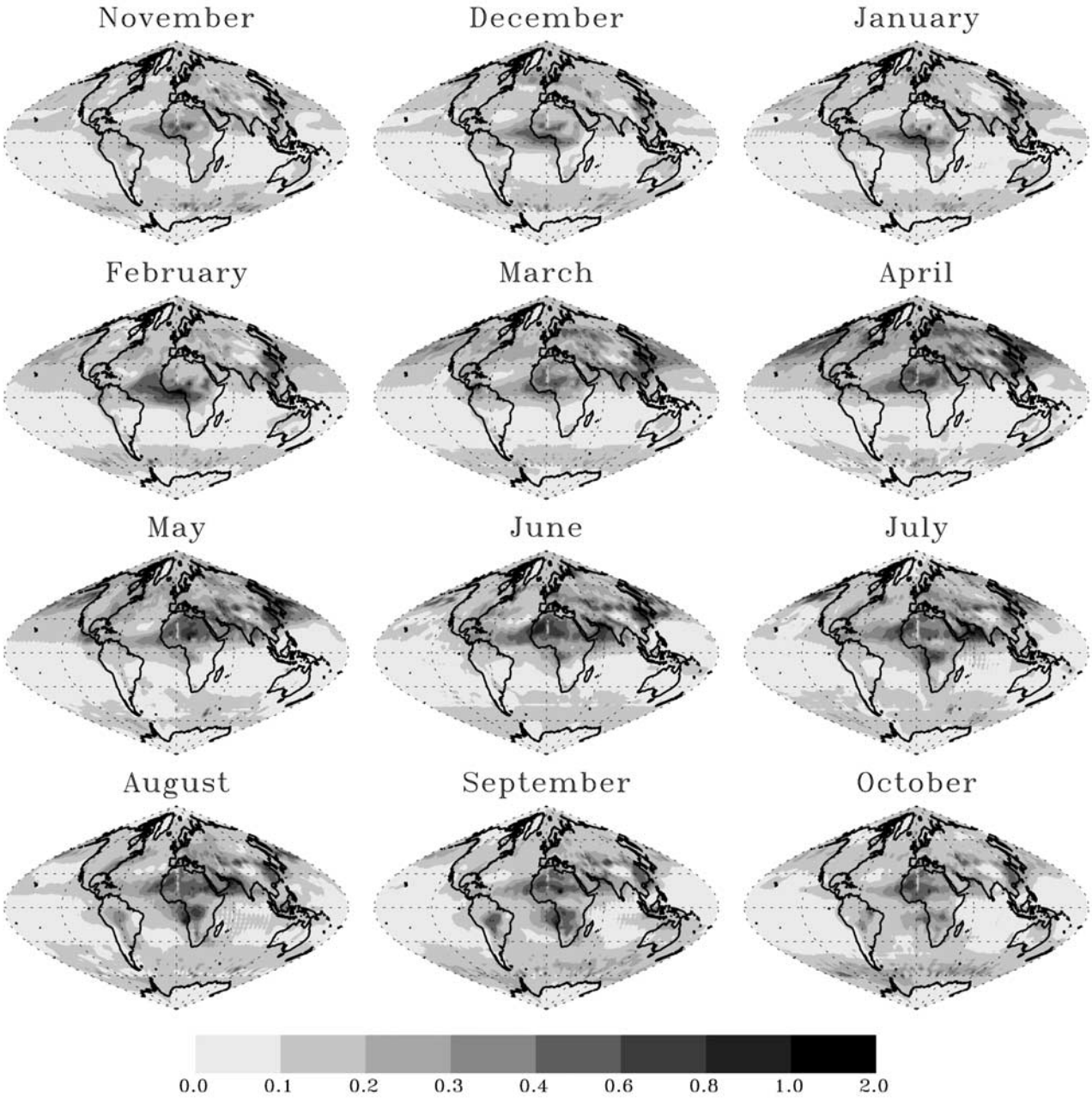

Figure 2. Assimilated annual cycle of aerosol optical depths at 550 nm based on MODIS retrievals and GOCART simulations from November 2000 to October 2001. See color version of this figure at back of this issue.

dust outbreaks extend as far as the tropical Atlantic, the southeast of North America, and the Arabian Sea.

2. East Asia and North Pacific. East Asia also has very high aerosol loading throughout the year, with the largest values of as much as 0.8 in eastern China in the spring. In northwestern China and Mongolia where mineral dusts originate, especially in spring, aerosol optical depths are relatively large. These springtime maxima in China are attributed to these dust outbreaks and also biomass burning from the southeast [*Herman et al.*, 1997; *Torres et al.*, 2002]. The Tibet Plateau is one of most pristine land areas in the world, with the aerosol optical depth of less than 0.1 in general. In the spring and early summer, aerosols and other air pollutants from East Asia are readily pumped up to high altitudes by intense frontal activities, and transported rapidly by the westerlies over the North Pacific and North America [e.g., *Merrill*, 1989; *Jacob et al.*, 1999; *Jeff et al.*, 1999]. Over the North Pacific, the aerosol optical depth reaches its maximum in spring and minimum in autumn, consistent with the seasonal variations detected by the AVHRR [*Husar et al.*, 1997]. The extremely large aerosol optical depth in the spring (e.g., more than 0.4 over the whole North Pacific in April) are further discussed in the next section.

3. West and South Asia. From March to September, the aerosol optical depth is more than 0.2. In spring, an aerosol optical depth of about 0.4 occurs over the Indian

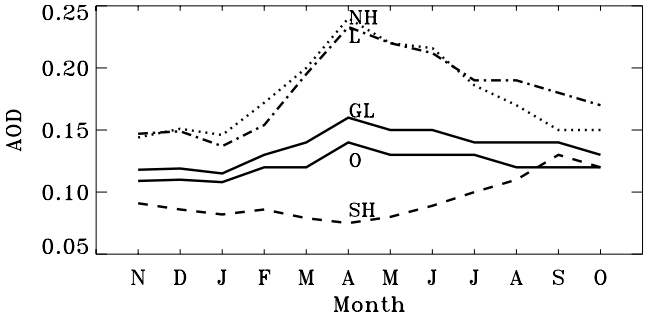

Figure 3. Monthly variations of the assimilated aerosol optical depths averaged over globe (GL), Northern Hemisphere (NH), Southern Hemisphere (SH), land (L), and ocean (O).

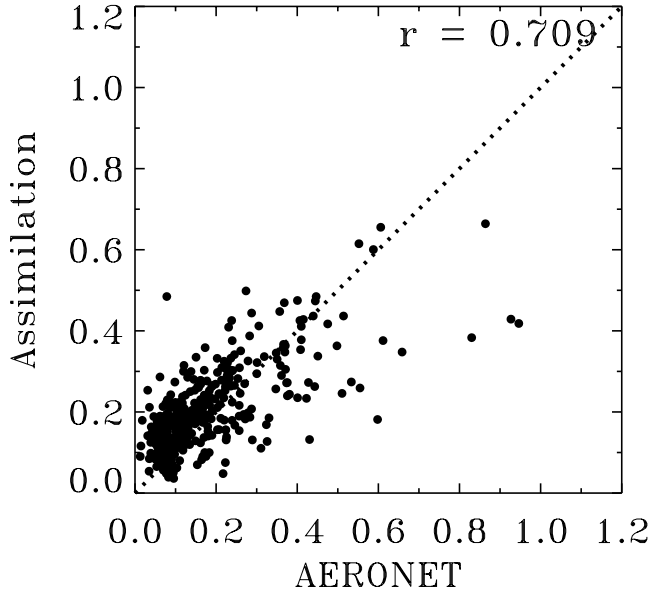

Figure 4. Correlation of the assimilated aerosol optical depths with the AERONET measurements from November 2000 to October 2001. The dotted line represents a 1:1 relationship.

subcontinent consistent with previous studies [e.g., *Collins et al.*, 2001] and in some other scattered areas. The transport of anthropogenic pollution by the winter monsoon from India to the Arabian Sea, leads to a large N-S contrast in the Indian Ocean. From June to August, aerosol optical depths are as high as 0.9 in the Arabian Sea, resulting from mineral dusts from Africa, the Arabian peninsula, and probably northern India. Similarly large values are also detected by AVHRR [*Husar et al.*, 1997] and TOMS [*Torres et al.*, 2002].

4. North America and Europe. The aerosol optical depth in eastern U.S. is about 0.2–0.4 in summer and spring months, and a factor of 2 smaller in winter months, a seasonality consistent with surface measurements in the region [e.g., *Malm et al.*, 1999]. In western U.S., the aerosol optical depth is mostly in the range of 0.1–0.2, but larger in April when Asian pollutants and dusts reach the continent from the North Pacific [*Jeff et al.*, 1999]. The aerosol loading over North America is on average more than a factor of 2 lower than that over China. Eastern Canada has a much larger aerosol optical depth in springtime (about 0.4) than in other seasons. The GOCART model simulates a factor of 2 smaller aerosol optical depth in this region than that from MODIS, with a major contribution from sulfate and minor contributions from sea-salt and dust. Forest fires are unlikely a reason for such large optical depths, as confirmed by the absence of absorbing aerosols in TOMS retrievals and small Angstrom exponent (less than 0.5) detected by MODIS. Asian dusts made small but detectable contributions in eastern North America [*Thulasiraman et al.*, 2002] and evidently are not a major reason for this. Further investigation is needed to sort out sources of such large optical depths. The aerosol optical depth over Europe is comparable to that over eastern US, except in the former USSR where the aerosol optical depth is larger, especially in spring.

5. Southern Hemisphere. Aerosol optical depths are lower than 0.2 in the Southern Hemisphere, except from June to October in South Africa and South America, corresponding to the peak of biomass burning and dry season in these regions [*Husar et al.*, 1997; *Torres et al.*, 2002]. For the period examined, the optical depths in South Africa are larger than those in South America. In August–October, biomass burning can be also active in Indonesia and tropical Australia. However, the aerosol optical depth in 2001 is not as large as that during the 1997 autumn biomass burning during a large El Niño event [*Nakajima et al.*, 1999]. The aerosol optical depth over most of the Southern Hemispheric oceans and over Antarctica are among the lowest (less than 0.05) in the world, except over the tropical/subtropical Atlantic Ocean where significant impacts of biomass burning from South Africa and South America occur in August–October, and over the 40°–60°S "roaring forties" band. The large aerosol optical depth in these latitudes is attributable to the large sea-salt production [e.g., *Chin et al.*, 2002] and also to possible contamination of the satellite measurements by whitecaps [*Higurashi and Nakajima*, 1999] and Sun glint (Kaufman, personal communication), both a result of the high winds.

[17] Figure 3 shows monthly variations of aerosol optical depths averaged over both hemispheres and the globe, land, and ocean. The annual mean of global aerosol optical depth is 0.134, ranging from 0.16 in April to about 0.12 in November. The average aerosol optical depths over the Northern Hemisphere and land have a larger seasonal variation than the global average, reaching its maximum

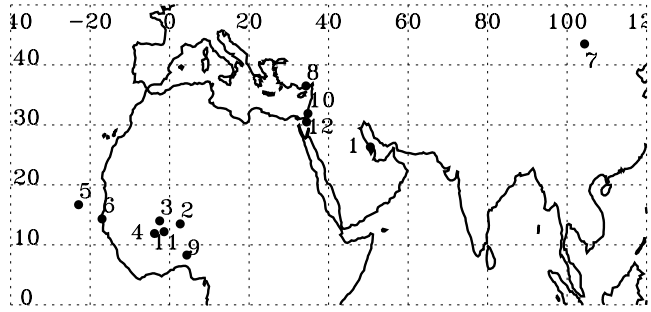

Figure 5. Locations of 12 near-desert AERONET sites in North Africa and West/Central Asia.

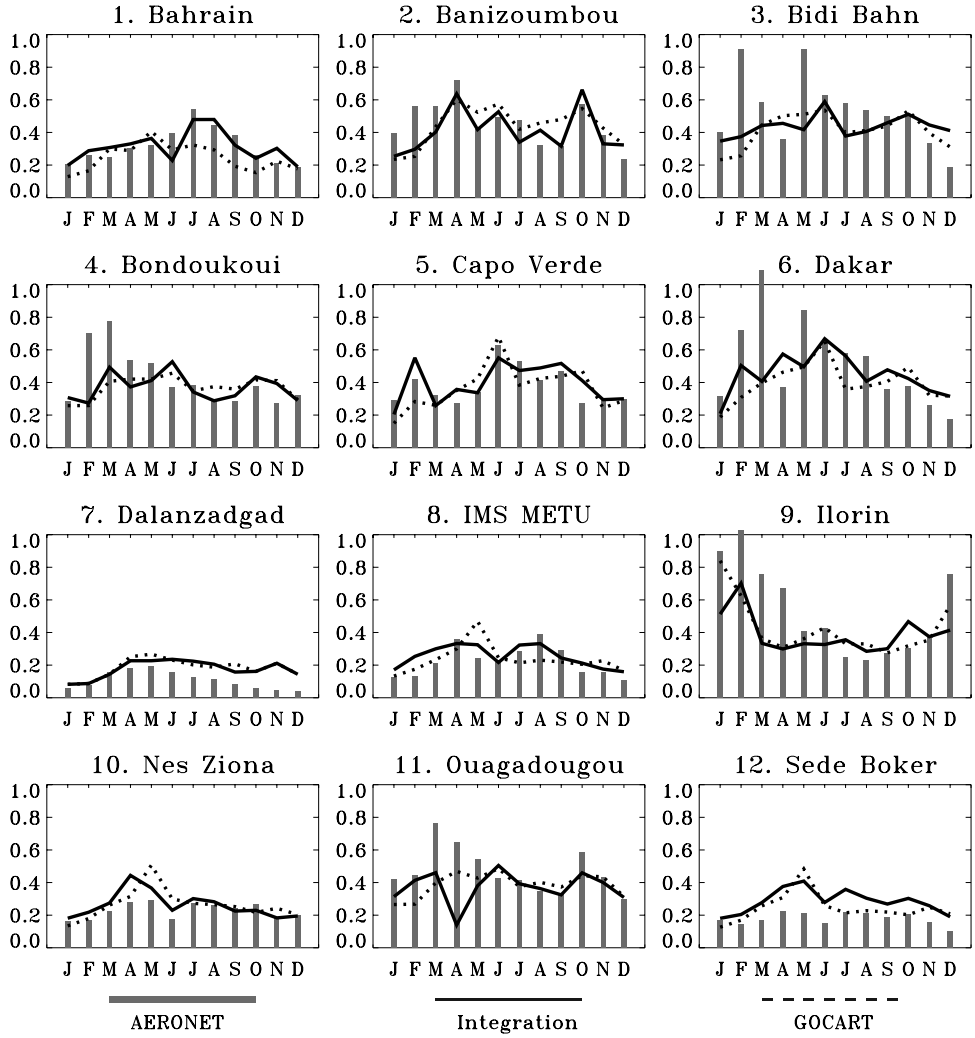

Figure 6. Comparisons of the annual cycle of the GOCART and assimilated aerosol optical depths with the AERONET aerosol climatology at 12 sites (located by numbers in Figure 5) in North Africa and West/Central Asia.

of about 0.23 in April and dropping to about 0.15 in Northern Hemispheric winter months. In the Southern Hemisphere, the aerosol optical depth is less than 0.1 before August and the largest aerosol optical depths occur in September and October when biomass burning is most intense. The aerosol optical depth over the oceans has a monthly variation similar to that of the global average.

4. Evaluation of the Aerosol Assimilation

[18] Figure 4 shows the correlation between the assimilated aerosol optical depths and the AERONET measurements corresponding to those in Figure 1. Overall, the combined data are better correlated with the AERONET measurements (a correlation coefficient of 0.71) than are either alone (see Figure 1). For low aerosol loading, the assimilation reduces most of extremely high biases in the MODIS data. At high loading, the AERONET τ is still higher, at least partially a result of the AERONET data being sampled in areas of urban maxima, as discussed earlier. *Ichoku et al.* [2002] used the MODIS 10 $\times$ 10 km optical depths to examine spatial variations of aerosols for several periods and locations, showing a small window-size dependence of area averages and no specific trend. Further investigation is needed to fully assess how the spatial variation and other sampling issues affect the correlation, which is beyond the scope of this study.

[19] The filling of missing MODIS data in arid and semiarid lands with model simulations is examined in terms of the annual cycle of aerosol assimilation for 12 near-desert AERONET stations in North Africa and West/Central Asia at locations shown in Figure 5. Figure 6 compares the annual cycle of GOCART and assimilated aerosol optical depth with the AERONET aerosol climatology (from 1993 onward with site-dependent durations) at these sites. The AERONET aerosol climatology is substituted for its incomplete annual cycle during 2001. The assimilation adequately reproduces the AERONET observed annual cycle. In regions of tropical Africa affected by both biomass burning and desert dust (sites 2–6, 9, and 11), the assimilated optical depths are generally smaller than those from the AERONET measure-

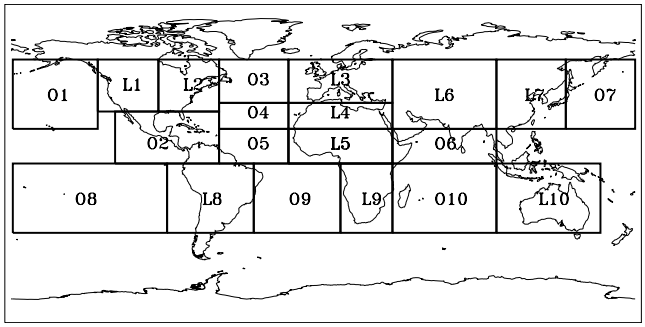

Figure 7. Illustration of 10 land regions (L1–L10) and 10 ocean regions (O1–O10) selected for regional comparisons of aerosol optical depths.

ments during the biomass burning season. On the other hand, for the Dalanzadgad and Sede Boker sites, the assimilated aerosol optical depths are significantly larger than those in the AERONET measurements for most months. Possible explanations for these differences include the interannual variability of biomass burning and dust outbreaks, potential biases resulting from local AERONET measurements not being regionally representative, and the model's underestimate of biomass burning but overestimate of dusts.

[20] To further assess the aerosol assimilation process, we compare the MODIS, GOCART, and assimilated aerosol optical depths for 10 land regions (numbering from L1 to L10) and 10 ocean regions (numbering from O1 to O10) as depicted in Figure 7. Figure 8 compares annual cycles of aerosol optical depths in the land regions, with the assimilated, MODIS, and GOCART aerosol optical depth denoted as solid, dotted, and dashed line, respectively. For the Saharan deserts (L4) and West/Central Asia (L6), MODIS retrievals are too scarce to give a regional average and hence are excluded from the plots. The assimilated aerosol optical depth in such regions generally follows the GOCART simulations. The well-defined summer peak in L4 agrees with that of previous studies [e.g., *Torres et al.*, 2002]. In North America (L1 and L2), the assimilated aerosol optical depth is generally close to that found by the MODIS retrieval but higher than that of the GOCART simulation. In western Europe (L3), the three data sets are in good agreement except for late spring and fall when the GOCART simulations are about 40% higher than the MODIS retrievals. In near-equatorial North Africa (L5) where both biomass burning and dust outbreaks contribute, the MODIS retrievals are generally higher than the GOCART simulations during the biomass burning season, but lower during the dust outbreaks. In East Asia (L7), the MODIS retrievals are 50–100% higher than the GOCART simulations from November to April, but the two match well in other months. Over land in the Southern Hemisphere (L8–L10), the MODIS retrievals are higher than the GOCART simulations by as much as a factor of 2, except during the biomass burning season over South Africa (L9) and South America (L8).

[21] Figure 9 shows a similar comparison for the ocean regions. The two-channel AVHRR aerosol optical depths at 550 nm are included, with the average denoted by dots and the observed range as vertical bars. Different data sets show similar monthly variations in all regions. The assimilated aerosol optical depth is generally in good agreement with the AVHRR retrievals over most oceans in the Northern Hemisphere (O2–O6) and over the South Atlantic (O9). Large discrepancies exist in the North Pacific (O1 and O7) and the remote South Pacific and South Indian Oceans (O8 and O10).

[22] Over the Northwest Pacific (O7) in spring and early summer, the MODIS aerosol optical depth is higher by a factor of 2 or so than are the model simulations and the AVHRR aerosol climatology. The same occurs in the Northeast Pacific (O1) in the spring. Although differences among retrieval algorithms may contribute, we propose that a major contribution would be from the extremely active transcontinental transport of Asian dust storms and pollutants in the spring of 2001. The GOCART may have underpredicted these events, although it has captured the AVHRR aerosol climatology very well. Meteorological conditions in spring are favorable for generating dust storms and for the fast eastward movement of large volumes of Asian air mass across the North Pacific [*Merrill*, 1989]. For example, well-documented intense dust storms and long-

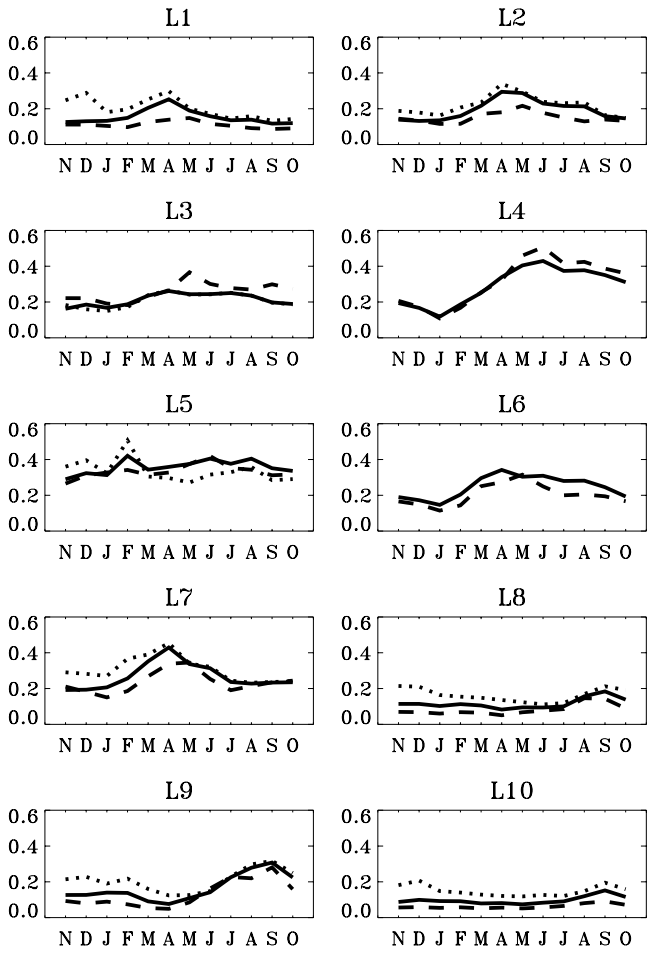

Figure 8. Comparisons of the assimilated (solid lines), MODIS (dotted lines), and GOCART (dashed lines) annual cycle of aerosol optical depths in 10 land regions (L1–L10). The label of x axis N, D, J, ..., S, and O denotes the month of November, December, January, ..., September, and October, respectively.

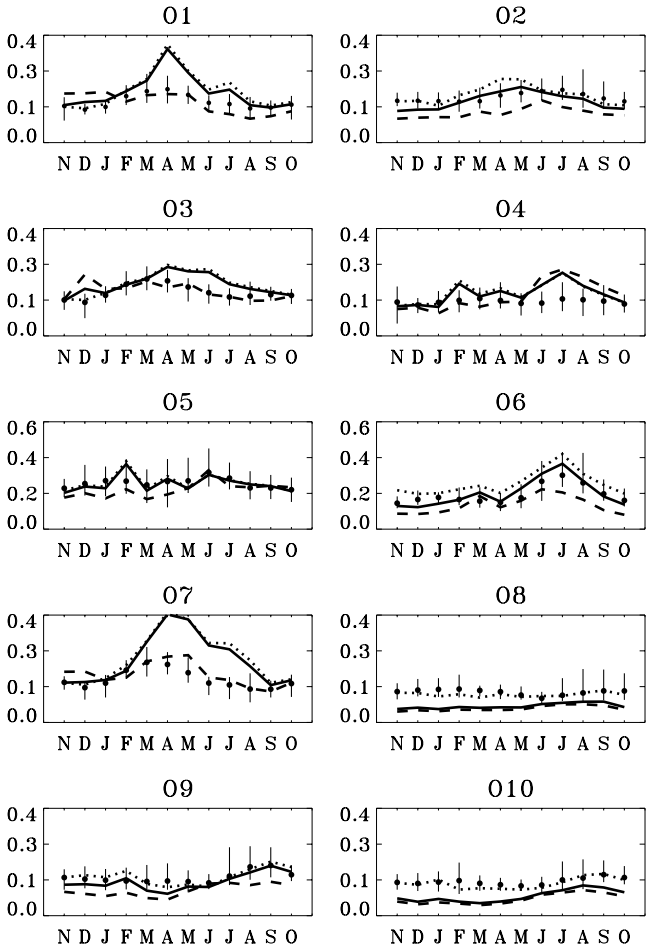

Figure 9. Comparisons of the assimilated (solid lines), MODIS (dotted lines), GOCART (dashed lines), and AVHRR (dots for average and vertical bars for the range) annual cycle of aerosol optical depths in 10 ocean regions (O1–O10). The label of *x* axis N, D, J, ..., S, and O denotes the month of November, December, January, ..., September, and October, respectively.

range transport occurred in April 1998 [*Husar et al.*, 2001]. Interannual variations of meteorology and hence of the uplifting of dusts and their intercontinnetal transport could be considerable [*Merrill*, 1989]. In fact, the Sea-viewing Wide Field-of-view Sensor (SeaWiFS) images showed unusually large and long-lasting dust clouds in April 2001 (NASA science news, 17 May 2001 at http://science.nasa.gov/headlines/). Dusts lifted by strong winds from the Gobi and Taklamakan deserts early in the month traveled very far eastward, drifting across the North Pacific, traversing North America and even reaching the mid-Atlantic late in the month. The unusual intensity and extent of the dust events are substantiated by the TOMS absorbing aerosol index data (ftp://toms.gsfc.nasa.gov/aerosols/aerosols.html) [*Herman et al.*, 1997; *Torres et al.*, 1998]. Figure 10 compares the composite of TOMS aerosol index for April between 2001 and 1998 in North Pacific Ocean. The composite aerosol index is averaged in regions where values greater than 0.4 have occurred for more than 5 days. Note that dust aerosol optical depth is proportional to the TOMS absorbing aerosol index. In April 2001, the whole North Pacific was blanketed with dust plumes, showing very small zonal variations. The dust storms in 2001 were more intense and dust was transported across the North Pacific for a much longer distance than occurred in the 1998 dust storm. There are three open-ocean AERONET sites at the south edge of intercontinental transport corridor detected by MODIS: Midway Island, 28°N, 177°W; Lanai, 20°N, 156°W; Coconut Island, 21°N, 157°W. The respective aerosol optical depths of 0.21, 0.11, and 0.12 at these sites also show good agreement with the MODIS retrievals.

[23] Over the remote South Pacific and South Indian Oceans (O8 and O10), the two satellite retrievals match very well, both being a factor of 2 higher than the GOCART simulations. In this context, GOCART behaves in a similar way to other global aerosol models examined by *Penner et al.* [2002]. Such discrepancies may be attributed to the uncertainties associated with both satellite retrievals and model simulations. Satellite retrievals still have difficulties in cloud screening and elimination of glint effects. The boxes O8 and O10 have close to the strongest surface winds in the Southern Hemisphere, as confirmed by the NCEP/NCAR reanalysis. The resultant whitecaps may have also

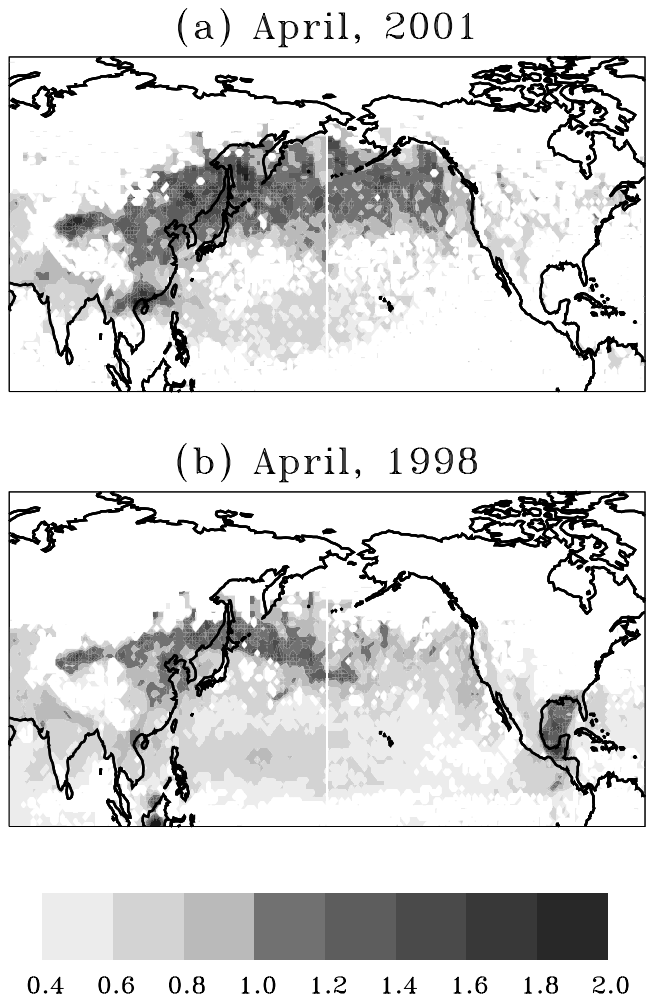

Figure 10. TOMS absorbing aerosol index for April in (a) 2001 and (b) 1998. The composite of aerosol index shown here is averaged in regions where values greater than 0.4 have occurred for more than 5 days.

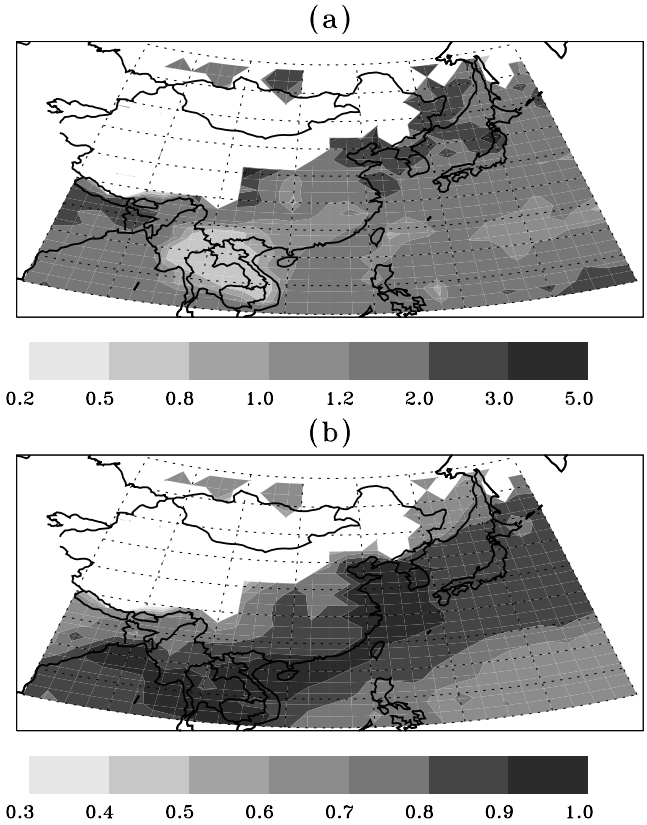

Figure 11. Distributions of (a) the MODIS/GOCART ratio for aerosol optical depth and (b) the fractional contribution of MODIS optical depth in the assimilation in East Asia for February 2001.

interfered with the MODIS retrievals. MODIS validations have shown relatively large uncertainties in remote areas [*Remer et al.*, 2002]. Model errors could also contribute to these large discrepancies. Anthropogenic emissions in the Indian subcontinent in 2001 are much higher than the 1990 or late 1980s emissions used in the GOCART model [*Chin et al.*, 2002]. This bias in emissions may partially explain the lower GOCART simulations over the tropical South Indian Ocean. *Penner et al.* [2002] speculated a missing non-sea-salt open-ocean source, and/or too low biomass burning emissions and DMS fluxes. It appears that uncertainties in biomass burning emissions are unlikely a reason for the discrepancies in these regions because they have no significant seasonal variations. The GOCART DMS results also compare quite well with the observations over the tropical Pacific [*Chin et al.*, 2000b], suggesting that the DMS flux would not be a major issue. The assimilated aerosol optical depths generally follow those simulated by the model in these remote oceans, a consequence of the assumed error parameters for model simulations as discussed earlier. The weight of MODIS optical depth and hence the assimilated optical depth increase with increasing fractional error of GOCART optical depth. Sensitivity tests show that, for a factor of 2 and 4 increase of fractional error coefficient (f_{mod}), the assimilated optical depths increase by about 20% and 40% respectively, but are still much smaller than the satellite retrievals. Evidently, uncertainties associated with the estimate of modeling errors are unlikely to fully explain the large differences between the assimilation and the AVHRR climatology.

5. Sensitivity to Assimilation Parameters

[24] Tests for East Asia (10°–55°N, 80°–150°E) examine the sensitivity of aerosol assimilation to the variation of assimilation parameters in Table 1. Figure 11 shows (a) the ratio of MODIS to GOCART aerosol optical depth and (b) the fractional contribution of MODIS τ in the standard assimilation for February 2001. MODIS retrievals are largely absent in western and part of northern China, and Mongolia, due to high surface reflection and/or persistent presence of clouds. Except in Laos and Thailand where the ratio of MODIS to GOCART optical depth is about 0.5, the MODIS aerosol optical depth is higher than that of the GOCART simulations. There is a belt with a MODIS/GOCART ratio of more than 2, which is close to the boundary of MODIS retrieval inclusion and extends from northeast of the domain down to northern India. In this belt and also the tropical Pacific, MODIS and GOCART make comparable contributions in the assimilation. The variance or relative weight of each product changes with statistical parameters, resulting in a change in the assimilation depending on the MODIS–GOCART discrepancies and the fractional contribution of each product. In the belt discussed above, a change of relative weight in combination with the large MODIS–GOCART discrepancies would give rise to a significant change in the assimilation. The term "sensitive belt" will be applied to such regions. For a small MODIS–GOCART difference, the change of relative weight will not significantly change the assimilation. In fact, no changes in the assimilation would occur where the two products are equal. When the assimilated optical depths are predominated by either MODIS or GOCART contributions, a change of variance or weight would not significantly change the relative contributions of individual products and hence the assimilation.

[25] Figure 12 shows the relative difference in the assimilated τ due to a factor of 2 decrease of the MODIS fractional error coefficient (f_{obs}). Decreases of f_{obs} from 0.2 (land) and 0.05 (ocean) to 0.1 and 0.025, respectively, bring the assimilated aerosol optical depths somewhat closer to the MODIS observations (a positive relative difference), because

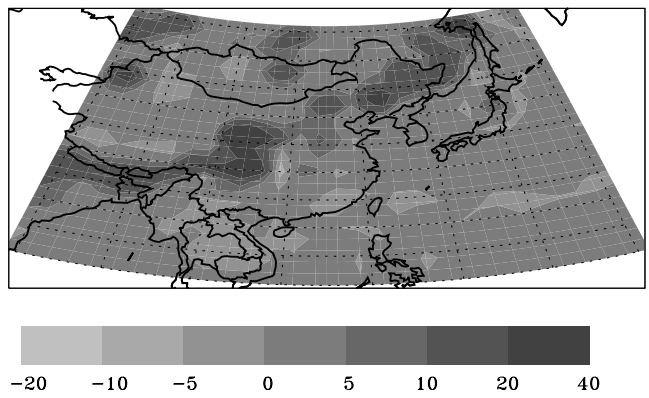

Figure 12. Relative differences (%) of the assimilated aerosol optical depth in East Asia for February 2001 by halving the fractional error of the MODIS aerosol optical depth (f_{obs}).

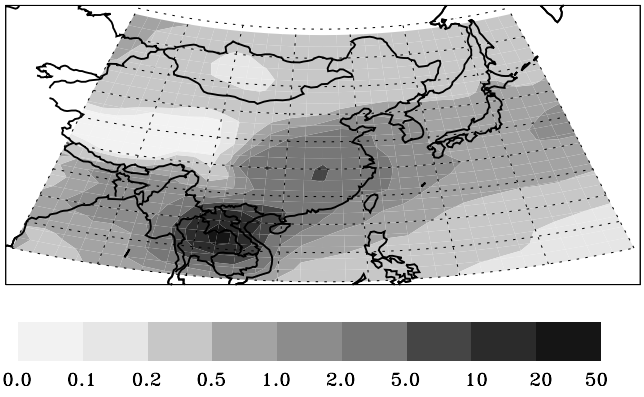

Figure 13. Distributions of GOCART optical depth variances ($\times 100$) with $f_{mod} = 0.5$ in East Asia for February 2001.

of the better accuracy and hence the larger weight given to the MODIS τ in the assimilation. Conversely, the optical depths shift toward those of the GOCART simulations when f_{obs} is doubled (not shown). In wide areas where either MODIS or GOCART dominates, such a change of f_{obs} does not significantly alter the relative contributions of MODIS and GOCART, introducing a difference of less than 5% in comparison to the standard assimilation. However, large relative difference of up to 30% occur in the "sensitive belt," because of comparable contributions by MODIS and GOCART and large MODIS–GOCART differences. The assimilation in the tropical Pacific is not sensitive to f_{obs}, though the MODIS and GOCART have relatively large differences and make comparable contributions to the assimilation. In this region, the MODIS optical depth is about 0.15 and according to Table 1, the weight or variance of MODIS optical depth is largely determined by the RMS error other than the fractional error.

[26] The differences due to the decrease (increase) of f_{mod} correspond to that due to the increase (decrease) of f_{obs}, respectively. For a factor of 2 decrease (from 0.50 to 0.25) or increase (from 0.50 to 1.0) in f_{mod}, the resultant percentage change is within 5% in wide areas but is up to about 30% in the "sensitive belt." In addition, the tropical Pacific also has a relatively large sensitivity to f_{mod}, different from the sensitivity to f_{obs}. A change of the minimum RMS error in MODIS τ (ϵ_{obs}) generally affects the assimilated τ by less than 5%. The largest uncertainty of about 15% occurs in the same "sensitive belt."

[27] The assimilation changes with L_{mx}, depending on the spatial pattern of GOCART variances as shown in Figure 13, in addition to the MODIS–GOCART difference and their fractional contributions. The larger the value and gradient of variances, the larger the sensitivity to L_{mx} is. Figure 14 depicts the relative difference in the assimilated aerosol fields that result from halving the L_{mx}. In the "sensitive belt," a factor of 2 decrease of L_{mx} increases the relative weight of GOCART to MODIS product and hence reduces the assimilation by 20–40% because the GOCART τ is about a factor of 2 smaller than the MODIS τ (Figure 11a). Although the GOCART contribution is small (about 10%) in Laos and Thailand, the considerably large values and gradients of variances result in a larger weight of GOCART τ and up to 50% increase in the assimilation when reducing the L_{mx}. In other regions, the relative difference is generally within 20%. A factor of 2 increase of L_{mx} gives a similar pattern to that in Figure 14 but with reversal of signs.

6. Concluding Remarks

[28] An optimum interpolation approach with Kalman filter has been applied to combine MODIS retrievals with GOCART simulations, hence generating an annual cycle of global aerosol optical depths at 550 nm for the period from November 2000 to October 2001.These aerosol optical depths have been evaluated against a large number of AERONET measurements over land and compared with the AVHRR aerosol climatology over ocean.

[29] The aerosol data set so generated captures the prominent features of geographical patterns and seasonal variations of aerosols as observed in previous studies. Among the highest aerosol loading regions are North Africa and East Asia, where biomass burning, industrial activities and/or dust outbreaks contribute. The large amount of aerosols imported from these regions to the tropical and subtropical Atlantic, and to the North Pacific, have significant and far-reaching impacts. The smallest aerosol optical depth occurs mainly over the South Pacific Ocean, the South Indian Ocean, Antarctica, the Tibetan Plateau, and Greenland. Pronounced seasonal variations include occurrence of dust storms in spring and summer in the Saharan desert and Arabian Peninsula, frequent spring dust outbreaks in northern China, springtime long-range transport of Asian aerosols over the North Pacific, and active biomass burning from July to October in the Southern Hemisphere.

[30] The assimilated aerosol optical depths are better correlated with the AERONET measurements than are either the MODIS retrievals or GOCART simulations alone. The coverage gap of MODIS retrievals in arid/semiarid lands is filled in with values that are generally consistent with the AERONET climatology. Over the oceans, the assimilation adequately reproduces the seasonal variations of AVHRR aerosol climatology, and over the Atlantic and North Indian Oceans, are in good agreement with the AVHRR climatology. However, over the North Pacific, the assimilated optical depth in the spring and early summer is much larger than that of the AVHRR climatology,

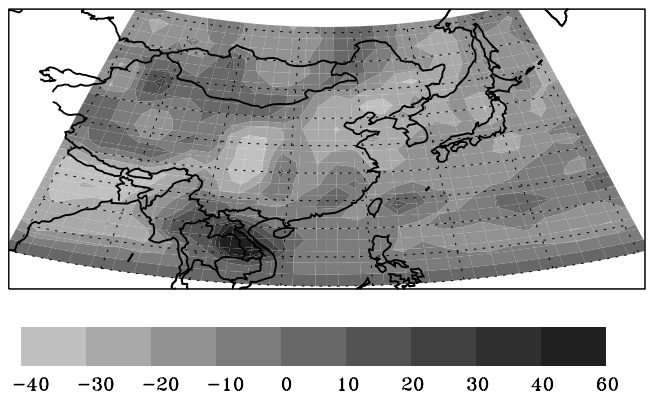

Figure 14. Relative differences (%) of the assimilated aerosol optical depth in East Asia for February 2001 by halving the horizontal correlation length for the error of GOCART aerosol optical depth (L_{mx}).

apparently primarily due to the occurrence of extremely intense and long-range transport of Asian dusts in 2001. In addition, the modeled and assimilated aerosol optical depths are much lower than those from the satellite retrievals over the South Pacific and South Indian Oceans. These differences may suggest an underestimation by the model in those regions, or overestimation by the satellite retrievals due to cloud, whitecap, and glint contamination, and a need of more realistic specification of error parameters.

[31] The assimilation is highly sensitive to the statistical parameters in regions where MODIS–GOCART discrepancies are large and the MODIS and GOCART contributions are comparable. Changes of up to 30–50% resulting from a factor of 2 change in the statistical parameters, suggests comparable levels of uncertainty. The uncertainties and/or biases associated with individual data sets will decrease with improved representation of aerosol processes in models, new satellite retrieval algorithms, and better estimates of statistical parameters. How to quantify and remove potential biases in the retrievals and simulations remains an open issue.

[32] **Acknowledgments.** We are grateful to Boris Khattatov and Jean-Francois Lamarque of NCAR for using their assimilation package developed for scientific programs sponsored by NASA and NCAR. Paul Ginoux of NASA/GSFC is acknowledged for contributing to GOCART model simulations. HY benefited much from discussions with William Collins and Phil Rasch of NCAR and Stefan Kinne, Lorraine Remer, Allen Chu, and Arlindo da Silva of NASA/GSFC. The authors also appreciate great endeavors by a large number of MODIS, AERONET, AVHRR, and TOMS scientists in collecting and processing data. The research was sponsored by the DOE SCIDAC project DE-FG02-01ER63198 and NASA IDS project. HY is grateful to the support from NASA AEROCENTER Visitor program. Mian Chin was supported by the NASA Radiation Science Program and Atmospheric Chemistry Modeling and Analysis Program (ACMAP). Insightful comments from reviewers are gratefully acknowledged.

References

Ackerman, A. S., O. B. Toon, D. E. Stevens, A. J. Heymsfield, V. Ramanathan, and E. J. Welton, Reduction of tropical cloudiness by soot, *Science*, *288*, 1042–1047, 2000.

Albrecht, B. A., Aerosols, cloud microphysics, and fractional cloudiness, *Science*, *245*, 1227–1230, 1989.

Bohren, C. F., and D. R. Huffman, *Absorption and Scattering of Light by Small Particles*, John Wiley, New York, 1983.

Chameides, W. L., et al., A case study of the effects of atmospheric aerosols and regional haze on agriculture: An opportunity to enhance crop yields in China through emission controls?, *Proc. Natl. Acad. Sci.*, *96*(24), 13,626–13,633, 1999.

Charlson, R. J., Extending atmospheric aerosol measurements to the global scale, in *Weather Forecasting to Exploring the Solar System*, edited by C. Boutron, pp. 67–81, EDP Sci., Les Ulis, France, 2000.

Charlson, R. J., S. E. Schwartz, J. H. Hales, R. D. Cess, J. A. Coakley Jr., J. E. Hansen, and D. J. Hofmann, Climate forcing by anthropogenic aerosols, *Science*, *255*, 423–430, 1992.

Chin, M., R. B. Rood, S.-J. Lin, J.-F. Muller, and A. M. Thompson, Atmospheric sulfur cycle simulated in the global model GOCART: Model description and global properties, *J. Geophys. Res.*, *105*, 24,671–24,687, 2000a.

Chin, M., D. L. Savoie, B. J. Huebert, A. R. Bandy, D. C. Thornton, T. S. Bates, P. K. Quinn, E. S. Saltzman, and W. J. De Bruyn, Atmospheric sulfur cycle simulated in the global model GOCART: Comparison with field observations and regional budgets, *J. Geophys. Res.*, *105*, 24,689–24,712, 2000b.

Chin, M., P. Ginoux, S. Kinne, O. Torres, B. Holben, B. N. Duncan, R. V. Martin, J. A. Logan, A. Higurashi, and T. Nakajima, Aerosol distributions and radiative properties simulated in the GOCART model and comparisons with observations, *J. Atmos. Sci.*, *59*, 461–483, 2002.

Chu, D. A., Y. J. Kaufman, C. Ichoku, L. A. Remer, D. Tanre, and B. N. Holben, Validation of MODIS aerosol optical depth retrieval over land, *Geophys. Res. Lett.*, *29*, doi:10.1029/2001GL013205, 2002.

Coakley, J. A., Jr., R. D. Cess, and F. B. Yurevich, The effect of tropospheric aerosols on the earth's radiation budget: A parameterization for climate models, *J. Atmos. Sci.*, *40*, 116–138, 1983.

Collins, W. D., P. J. Rasch, B. E. Eaton, B. V. Khattatov, J.-F. Lamarque, and C. S. Zender, Simulating aerosols using a chemical transport model with assimilation of satellite aerosol retrievals: Methodology for INDOEX, *J. Geophys. Res.*, *106*, 7313–7336, 2001.

Delmas, R. A., P. Loudjani, A. Podaire, and J.-C. Menaut, Biomass burning in Africa: An assessment of annually burned biomass, in *Global Biomass Burning: Atmospheric, Climatic, and Biospheric Implications*, edited by J. S. Levine, pp. 126–132, MIT Press, Cambridge, Mass., 1991.

Dickerson, R. R., et al., The impacts of aerosols on solar ultraviolet radiation and photochemical smog, *Science*, *278*, 827–830, 1997.

Dubovik, O., B. N. Holben, T. F. Eck, A. Smirnov, Y. J. Kaufman, M. D. King, D. Tanre, and I. Slutsker, Variability of absorption and optical properties of key aerosol types observed in worldwide locations, *J. Atmos. Sci.*, *59*, 590–608, 2002.

Geogdzhayev, I. V., M. I. Mishchenko, W. B. Rossow, B. Cairns, and A. A. Lacis, Global two-channel AVHRR retrievals of aerosol properties over the ocean for the period of NOAA-9 observations and preliminary retrievals using NOAA-7 andNOAA-11 data, *J. Atmos. Sci.*, *59*, 262–278, 2002.

Ginoux, P., M. Chin, I. Tegen, J. Prospero, B. Holben, O. Dubovik, and S.-J. Lin, Sources and distributions of dust aerosols simulated with the GOCART model, *J. Geophys. Res.*, *106*, 20,225–20,273, 2001.

Hansen, J., M. Sato, and R. Ruedy, Radiative forcing and climate response, *J. Geophys. Res.*, *102*, 6831–6864, 1997.

Haywood, J., and O. Boucher, Estimates of the direct and indirect radiative forcing due to tropospheric aerosols: A review, *Rev. Geophys.*, *38*, 513–543, 2000.

Hegg, A., The impact of clouds on aerosol population, *IGACtivities 23*, April 2001.

Heintzenberg, J., H.-F. Graf, R. J. Charlson, and P. Warneck, Climate forcing and the physico-chemical life cycle of the atmospheric aerosol: Why do we need an integrated, interdisciplinary global research programme?, *Beitr. Phys. Atmos.*, *69*, 261–271, 1996.

Herman, J. R., P. K. Bhartia, O. Torres, C. Hsu, C. Seftor, and E. Celarier, Global distribution of UV-absorbing aerosols from Nimbus-7/TOMS Data, *J. Geophys. Res.*, *102*, 16,911–16,922, 1997.

Higurashi, A., and T. Nakajima, Development of a two channel aerosol retrieval algorithm on global scale using NOAA/AVHRR, *J. Atmos. Sci.*, *56*, 924–941, 1999.

Holben, B. N., et al., AERONET: A federated instrument network and data archive for aerosol characterization, *Remote Sens. Environ.*, *66*, 1–16, 1998.

Holben, B. N., et al., An emerging ground-based aerosol climatology: Aerosol optical depth from AERONET, *J. Geophys. Res.*, *106*, 12,067–12,098, 2001.

Husar, R. B., J. M. Prospero, and L. L. Stowe, Characterization of tropospheric aerosols over the oceans with the NOAA advanced very high resolution radiometer optical thickness operational product, *J. Geophys. Res.*, *102*, 16,889–16,909, 1997.

Husar, R. B., et al., Asian dust events of April 1998, *J. Geophys. Res.*, *106*, 18,317–18,330, 2001.

Ichoku, C., et al., A spatio-temporal approach for global validation and analysis of MODIS aerosol products, *Geophys. Res. Lett.*, *29*, 10.1029/2001GL013206, 2002.

Ignatov, A. M., L. L. Stowe, R. R. Singh, D. Kabanov, and I. Dergileva, Validation of NOAA/AVHRR retrievals using sun-photometer measurements from RV Akademik Vernadsky in 1991, *Adv. Space Res.*, *16*(10), 95–98, 1995.

Jacob, D. J., J. A. Logan, and P. P. Murti, Effect of rising Asian emissions on surface ozone in the United States, *Geophys. Res. Lett.*, *26*, 2175–2178, 1999.

Jeff, D. A., et al., Transport of Asian air pollution to North America, *Geophys. Res. Lett.*, *26*, 711–714, 1999.

Kaufman, Y. J., D. Tanre, L. A. Remer, E. F. Vermote, A. Chu, and B. N. Holben, Operational remote sensing of tropospheric aerosol over land from EOS moderate resolution imaging spectroradiometer, *J. Geophys. Res.*, *102*, 17,051–17,067, 1997.

Kaufman, Y. J., B. N. Holben, D. Tanre, I. Slutsker, A. Smirnov, and T. F. Eck, Will aerosol measurements from Terra and Aqua polar orbiting satellites represent the daily aerosol abundance and properties?, *Geophys. Res. Lett.*, *27*, 3861–3864, 2000.

Kaufman, Y. J., D. Tanre, and O. Boucher, A satellite view of aerosols in the climate system, *Nature*, *419*, 10.1038/nature01091, 2002.

Khattatov, B. V., J. C. Gille, L. V. Lyjak, G. P. Brasseur, V. L. Dvortsov, A. E. Roche, and J. Waters, Assimilation of photochemically active species and a case analysis of UARS data, *J. Geophys. Res.*, *104*, 18,715–18,737, 1999.

Khattatov, B. V., J.-F. Lamarque, L. V. Lyjak, R. Menard, P. Levelt, X. Tie, G. P. Brasseur, and J. C. Gille, Assimilation of satellite observations

of long-lived chemical species in global chemistry transport models, *J. Geophys. Res.*, *105*, 29,135–29,144, 2000.
Kiehl, J. T., and B. P. Briegleb, The relative role of sulfate aerosols and greenhouse gases in climate forcing, *Science*, *260*, 311–314, 1993.
King, M. D., Y. J. Kaufman, D. Tanre, and T. Nakajima, Remote sensing of tropospheric aerosols from space: Past, present and future, *Bull. Am. Meteorol. Soc.*, *80*, 2229–2259, 1999.
Lamarque, J.-F., B. V. Khattatov, and J. C. Gille, Assimilation of Measurement of Air Pollution from Space (MAPS) CO in a global three-dimensional model, *J. Geophys. Res.*, *104*, 26,209–26,218, 1999.
Levelt, P. F., B. V. Khattatov, J. C. Gille, G. P. Brasseur, X. X. Tie, and J. Waters, Assimilation of MLS ozone measurements in the global three-dimensional chemistry-transport model ROSE, *Geophys. Res. Lett.*, *25*, 4493–4496, 1998.
Lorenc, A. C., Analysis methods for numerical weather prediction, *Q. J. R. Meteorol. Soc.*, *112*, 1177–1194, 1986.
Malm, W. C., J. F. Sisler, D. Huffman, R. A. Eldred, and T. A. Cahill, Spatial and seasonal trends in particle concentration and optical extinction in the United States, *J. Geophys. Res.*, *99*, 1347–1370, 1999.
Merrill, J. T., Atmospheric long-range transport to the Pacific Ocean, in *Chemical Oceanography*, vol. 10, edited by J. P. Riley, R. Chester, and R. A. Duce, pp. 15–50, Academic, San Diego, Calif., 1989.
Mishchenko, M. I., I. V. Geogdzhayev, B. Cairns, W. B. Rossow, and A. A. Lacis, Aerosol retrievals over the ocean by use of channels 1 and 2 AVHRR data: Sensitivity analysis and preliminary results, *Appl. Opt.*, *38*(36), 7325–7341, 1999.
Nakajima, T., A. Hingurashi, N. Takeuchi, and J. R. Herman, Satellite and ground-based study of optical properties of 1997 Indonesian forest fire aerosols, *Geophys. Res. Lett.*, *26*, 2421–2424, 1999.
Penner, J. E., R. E. Dickinson, and C. A. O'Neill, Effects of aerosol from biomass burning on the global radiation budget, *Science*, *256*, 1432–1434, 1992.
Penner, J. E., et al., Quantifying and minimizing uncertainty of climate forcing by anthropogenic aerosols, *Bull. Am. Meteorol. Soc.*, *75*, 375–400, 1994.
Penner, J. E., et al., A comparison of model- and satellite derived aerosol optical depth and reflectivity, *J. Atmos. Sci.*, *59*, 441–460, 2002.
Ramanathan, V., P. J. Crutzen, J. L. Kiehl, and D. Rosenfeld, Aerosols, climate, and the hydrological cycle, *Science*, *294*, 2119–2124, 2001.
Rasch, P. J., W. D. Collins, and B. E. Eaton, Understanding the Indian Ocean Experiment (INDOEX) aerosol distributions with an aerosol assimilation, *J. Geophys. Res.*, *106*, 7337–7355, 2001.
Remer, L. A., et al., Validation of MODIS aerosol retrieval over ocean, *Geophys. Res. Lett.*, *29*, doi:10.1029/2001GL013204, 2002.
Rosenfeld, D., TRMM observed first direct evidence of smoke from forest fires inhibiting rainfall, *Geophys. Res. Lett.*, *26*, 3105–3108, 1999.
Rosenfeld, D., Suppression of rain and snow by urban and industrial air pollution, *Science*, *287*, 1793–1796, 2000.
Sato, M., J. E. Hansen, M. P. McCormick, and J. B. Pollack, Stratospheric aerosol optical depth, 1850–1990, *J. Geophys. Res.*, *98*, 22,987–22,994, 1993.
Tanre, D., Y. J. Kaufman, M. Herman, and S. Mattoo, Remote sensing of aerosol properties over oceans using the MODIS/EOS spectral radiances, *J. Geophys. Res.*, *102*, 16,971–16,988, 1997.
Thulasiraman, S., et al., Sunphotometric observations of the 2001 Asian dust storm over Canada and the U.S., *Geophys. Res. Lett.*, *29*, doi:10.1029/2001GL014188, 2002.
Torres, O., P. K. Bhartia, J. R. Herman, Z. Ahmad, and J. Gleason, Derivation of aerosol properties from satellite measurements of backscattered ultraviolet radiation: Theoretical basis, *J. Geophys. Res.*, *103*, 17,099–17,110, 1998.
Torres, O., P. K. Bhartia, J. R. Herman, A. Sinyuk, P. Ginoux, and B. Holben, A long-term record of aerosol optical depth from TOMS observations and comparison to AERONET measurements, *J. Atmos. Sci.*, *59*, 398–413, 2002.
Twomey, S., The influence of pollution on the shortwave albedo of clouds, *J. Atmos. Sci.*, *34*, 1149–1152, 1977.
Yu, H., S. C. Liu, and R. E. Dickinson, Radiative effects of aerosols on the evolution of the atmospheric boundary layer, *J. Geophys. Res.*, *107*, 4142, doi:10.1029/2001JD000754, 2002.

M. Chin, R. E. Dickinson, and H. Yu, School of Earth and Atmospheric Sciences, Georgia Institute of Technology, Atlanta, GA 30332, USA. (yu@breeze.eas.gatech.edu)
I. V. Geogdzhayev and M. I. Mishchenko, NASA Goddard Institute for Space Studies, 2880 Broadway, New York, NY 10025, USA.
B. N. Holben, Biospheric Sciences Branch, Code 923, NASA Goddard Space Flight Center, Greenbelt, MD 20771, USA.
Y. J. Kaufman, Laboratory for Atmospheres, Code 913, NASA Goddard Space Flight Center, Greenbelt, MD 20771, USA.

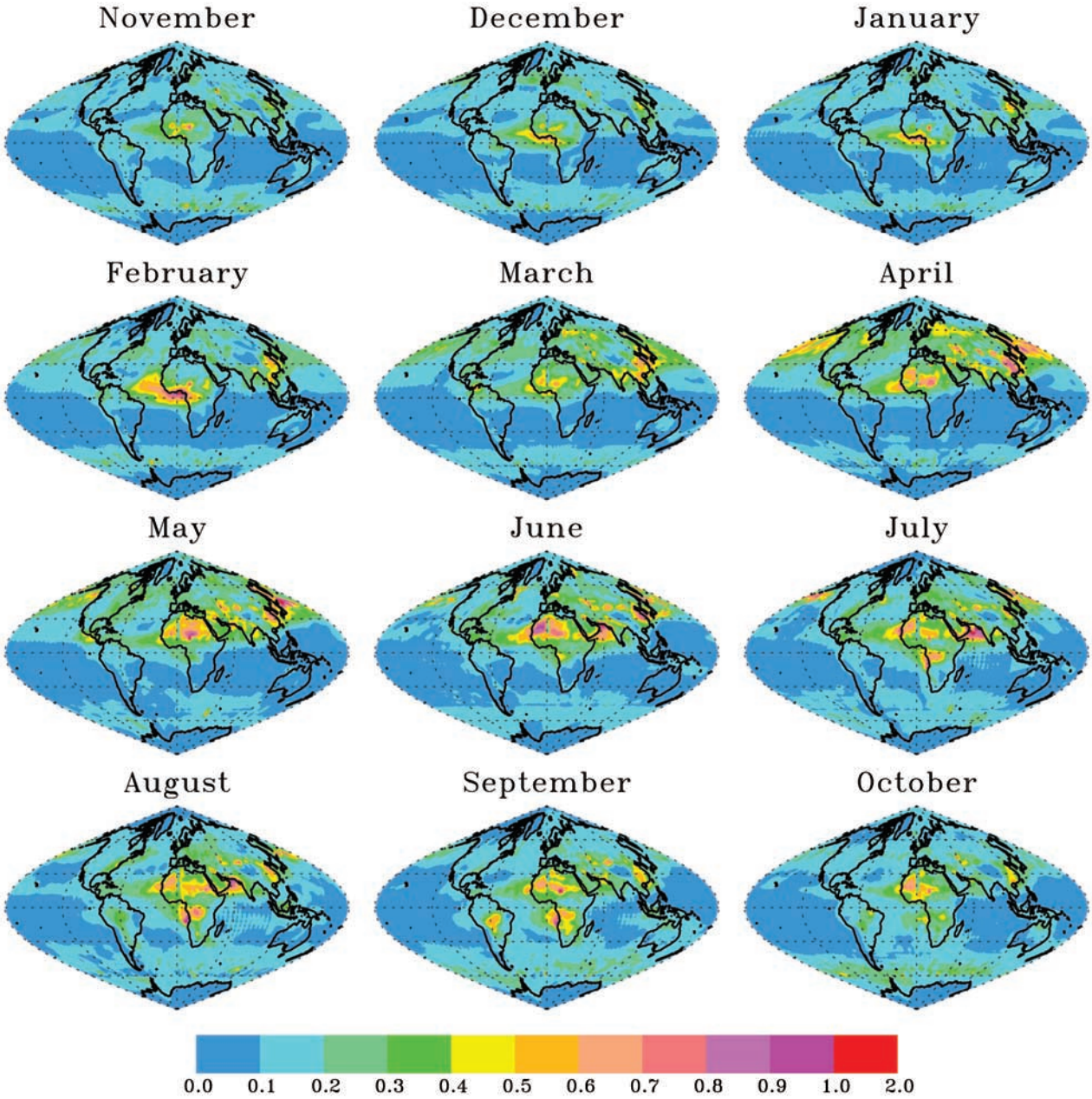

Figure 2. Assimilated annual cycle of aerosol optical depths at 550 nm based on MODIS retrievals and GOCART simulations from November 2000 to October 2001.